Composite Structures 93 (2011) 3104–3111

Contents lists available at ScienceDirect

Composite Structures

journal homepage: www.elsevier.com/locate/compstruct

Pyramidal lattice sandwich structures with hollow composite trusses

Sha Yin [a], Linzhi Wu [a,*], Li Ma [a], Steven Nutt [b]

[a] Center for Composite Materials, Harbin Institute of Technology, Harbin 150001, China
[b] Department of Chemical Engineering and Materials Science, University of Southern California, Los Angeles, CA 90089-0241, USA

ARTICLE INFO

Article history:
Available online 1 July 2011

Keywords:
Carbon fibers
Lattice structure
Hollow truss
Failure mode
Compressive properties
Energy absorption

ABSTRACT

Pyramidal lattice sandwich structures with hollow composite trusses were fabricated using a thermal expansion molding approach. Composite lattice structures with three relative densities were fabricated with two fiber architectures and the out-of-plane compression properties were measured and compared. Lattice cores with a fraction of carbon fibers circumferentially wound around the hollow trusses (Variant 2) exhibited superior mechanical properties compared with similar structures comprised of unidirectional fibers (Variant 1). The out-of-plane compressive properties of composite pyramidal lattice structures in Variant 2 were well-matched by analytical predictions. Unusual strain hardening behavior was observed in the plateau region for Variant 2, and the energy absorption capabilities were measured and compared with the similarly constructed silicone rubber–core truss pyramidal lattice structures (Variant 3). The energy absorption per unit mass of selected hollow truss composite lattice structures reported here surpassed that of both hybrid truss counterparts (Variant 3) and hollow truss metallic lattice structures.

1. Introduction

Sandwich structures consisting of two solid face sheets and a low-density porous core are widely used in weight-critical structural applications. The wide variety of sandwich structures stems largely from the diversity of sandwich core topologies and the variation of the component materials. Sandwich cores range from stochastic cellular materials, such as metallic and polymeric foams, to periodic lattice materials. Lattice materials are efficient, stretch-dominated structures well-suited to multifunctional applications [1]. Metallic lattice structures have been produced with a variety of topologies such as tetrahedral [2,3], pyramidal [4,5], Kagome [6] and hollow truss lattice [7–9].

Recent attention has been directed to composite truss cores, which are actually hybrids of composite materials with optimal lattice topology [10–16]. These novel engineering structures are expected to fill gaps in the material property space. Multiple techniques have been employed to fabricate composite lattice structures, such as hot press molding [15,16] and interlocking [12,13], both of which show promise for future application. However, there are few reports describing fabrication methods for composite lattice structures comprised of hollow trusses.

Metallic pyramidal lattice structures have been constructed with hollow trusses, resulting in greater inelastic buckling collapse strength than their solid truss counterparts [8]. Hollow trusses exhibit greater buckling resistance than solid trusses because of the greater second area moments. Moreover, the relative density of those pyramidal lattice structures is readily adjusted by varying the truss wall thickness without changing the cell size or truss slenderness ratio [8,9].

In the present study, a thermal expansion molding approach was developed for producing pyramidal lattice structures comprised of hollow composite trusses. Composite lattice structures with three relative densities were fabricated with two fiber architectures, and the out-of-plane compressive properties were measured. Analytical predictions of compressive properties were carried out and compared with experimental data. Finally, energy absorption capacity was explored for selected hollow truss composite pyramidal lattice structures, and the results were compared with those of the corresponding hybrid truss counterparts and other competing lattice structures.

2. Fabrication

A thermal expansion molding approach was developed and used to fabricate pyramidal lattice structures with hollow composite trusses. Female steel molds and male molds of silicone rubber are employed. The female molds are assemblies of multiple identical and interchangeable unit molds (Fig. 1a). To simplify the demoulding process, each unit mold is divided into three parts. The unit mold contains multiple semicylindrical surface grooves, and when matches with a second unit mold, these grooves form arrays of cylindrical cavities (Fig. 1a).

* Corresponding author. Tel.: +86 451 86412549; fax: +86 451 86402379.
E-mail address: wlz@hit.edu.cn (L. Wu).

0263-8223/$ - see front matter © 2011 Elsevier Ltd. All rights reserved.
doi:10.1016/j.compstruct.2011.06.025

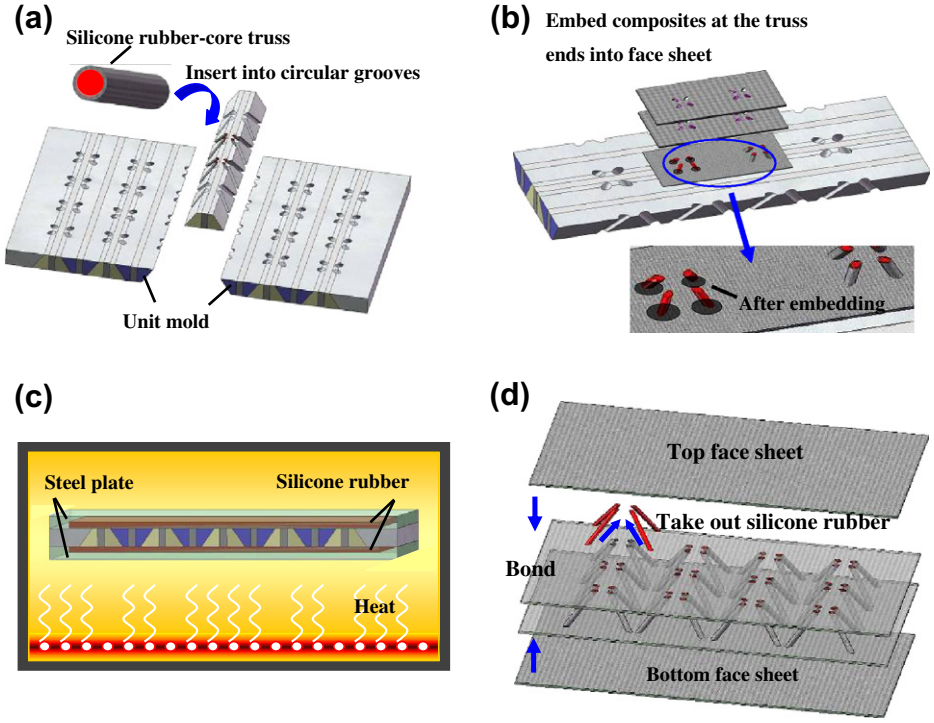

Fig. 1. Illustration of the fabrication approach for pyramidal lattice core sandwich structures with CF composite hollow trusses.

Both unidirectional prepreg (3234/T700) and plain weave fabric prepreg (3234/G803) (Beijing Institute of Aeronautical Materials, China) were used as parent materials. Pyramidal lattice structures with hollow composite trusses were fabricated in four steps. First, carbon fiber (CF) prepregs were stacked in a pre-designed sequence, then wrapped around silicone rubber rods to form hybrid trusses and inserted into the cylindrical cavities of the assembled steel molds (Fig. 1a), about 5 mm higher than the mold surface at each end. Second, plies of perforated CF prepreg were prepared with holes to match the truss positions and laid over the hybrid trusses, and the CF composite shells at the ends of each hybrid truss were peeled from the rubber rods and embedded between two plies of the perforated prepreg (Fig. 1b). Next, unidirectional prepregs (similarly perforated) were overlaid and stacked as face sheets on the top and bottom surfaces of the steel molds, and the excess silicone rubber in each hybrid truss was removed. Finally, the assembly was sandwiched between two steel plates filled with silicone rubber and placed in an oven for curing at 125 °C for 2 h (Fig. 1c). During curing, the silicone rubber in the steel molds and the plates expanded, providing compaction pressure for both face sheets and trusses. After curing, both the female and male molds were removed, and the composite structure with hollow trusses was bonded to two solid CF face sheets using an epoxy adhesive (J263, Heilongjiang Institute of Petrochemical), as illustrated in Fig. 1d.

2.1. Relative density

A typical pyramidal lattice structure with hollow composite trusses is shown in Fig. 2, and a representative unit cell is sketched in Fig. 3. The relative density ($\bar{\rho}_h$) is defined as the density of pyramidal lattice truss core (ρ_c) divided by that of the hollow truss (ρ_s) from which it is comprised

$$\bar{\rho}_h = \frac{\rho_c}{\rho_s} = \frac{\pi\left(d_o^2 - d_i^2\right)}{\sin\omega\left(\sqrt{2}l_1\cos\omega + 2l_2\right)^2} \tag{1}$$

where d_o and d_i are the outer and inner diameters of hollow trusses, l_1 is the truss length, ω is the inclination angle between the truss members and the base of the unit cell, and l_2 represents the side length of the square at the top of a pyramidal core. Here, d_o = 6 mm, l_1 = 19.8 mm, ω = 45°, and l_2 = 15 mm. The inner diameter, d_i, is roughly equal to that of the rubber rods used for fabrication, and three rod sizes were used with diameters of 5.4 mm, 4.5 mm, and 3 mm. The relative density was readily controlled without changing the cell size simply by varying the diameter of the rubber rods. The predicted relative densities generally should be greater than the measured densities, because the thermal expansion of the silicone rubber during curing increases the inner diameter of the hollow trusses (see Table 1).

Fig. 2. Pyramidal lattice sandwich structure with hollow composite trusses fabricated by thermal expansion molding process.

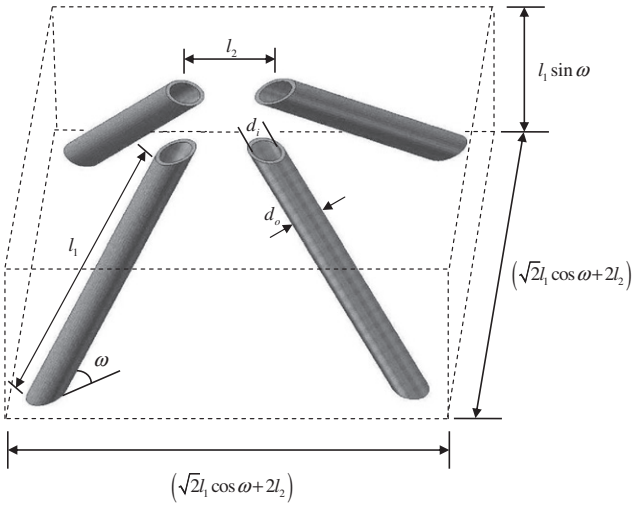

Fig. 3. Unit cell of a pyramidal lattice structure with hollow trusses.

2.2. Processing factor

The processing pressure at the gel temperature T is critical to the mechanical properties of composite tube trusses, and can be expressed as

$$P = K_V \frac{\Delta V}{V} \tag{2.1}$$

where

$$\begin{aligned} V &= \pi l_1 d_i^2 [1 + \alpha_V (T - T_0)]/4 \\ V' &= \pi l_1 d_i'^2/4 \\ \Delta V &= V - V' \end{aligned} \tag{2.2}$$

The processing pressure can be expressed in the following form

$$P = K_V \left\{ 1 - \frac{d_i'^2}{d_i^2 [1 + \alpha_V (T - T_0)]} \right\} \tag{3}$$

Here, α_V and K_V are the bulk expansion coefficient and modulus of silicone rubber, T_0 is the room temperature before processing, V is the volume of silicone rubber after free expansion in the gel state, V' is the final volume after processing with the corresponding actual inner diameter d_i' and ΔV is the increase in volume due to temperature variation. The parameter d_i' is determined from the process gap in the steel molds, which is difficult to control for these mm-scale trusses. The processing pressure is related to the thermal expansion properties of silicone rubber. Thus, the mechanical properties of these pyramidal lattice structures will be influenced by the selections of the silicone rubber and the associated characteristics.

3. Compressive properties

The compressive properties of pyramidal lattice structures were strongly dependent on the properties of the composite truss members, as expected. Out-of-plane compression tests were carried out on pyramidal lattice structures with hollow trusses fabricated with different stacking sequences using a screw-driven testing machine (INSTRON 5569, INSTRON, USA). These structures were compressed at a displacement rate of 0.5 mm/min at room temperature between two steel compression platens according to ASTM C365/C364M-05 [17].

3.1. Variant 1

Based on prior work, the compressive strength of composite lattice structures was expected to be greatest with unidirectional CF oriented along the truss member [16]. The stacking sequence in each hollow truss member of the pyramidal lattice structures fabricated here was $[0]_n$, where 0 represents the CF-truss axis angle, and n represents the number of plies. Here, three uni-truss wall thicknesses were produced using layups of $[0]_2$, $[0]_5$ and $[0]_{10}$, corresponding to rubber rod diameters of 5.4 mm, 4.5 mm and 3 mm and measured relative densities of 1.1%, 2.3%, and 4.75%.

The stress–strain behavior of these three variants (1a–c) of hollow truss lattice structures is shown in Fig. 4a. The curves reflect typical characteristics of pyramidal lattice sandwich structures comprised of CF composites, as reported previously [15,16]. In particular, the structures showed linear elastic behavior initially, reaching a peak stress at relatively small strain (~0.02–0.08). The peak was followed by a sharp stress drop associated with longitudinal splitting of composite struts (Fig. 4b), and progressive crushing. As longitudinal splitting occurred, the load transfer capacity of the matrix was compromised, and the load-carrying capacity of the CF was greatly diminished. This phenomenon occurred because there were no circumferential (hoop) fibers to resist transverse strains associated with buckling and Poisson expansion.

3.2. Variant 2

A second variant was fabricated based on a design that incorporated fiber orientations to resist hoop stresses in the truss tubes. CF/epoxy plain weave prepreg (3234/G814) was selected and added to the truss layups to produce three variants based on the following stacking sequences: $[(0, 90)]$, $[0_2/(0, 90)]$ and $[0_4/(0, 90)_2]$. These three variants (2a–c) resulted in relative densities of 1.07%, 2.21%, and 4.53%, respectively.

The compressive stress–strain behavior of Variants 2a–c is shown in Fig. 5a. The structures exhibited characteristics similar to those of Variant 1, including an initial elastic response, reaching a peak strength associated with truss fracture (Fig. 5b), followed by a stress drop and a long stress plateau, and finally a densification hardening region which began at a densification strain of 55–65% in Variant 2. However, the stress level here in the stress plateau period is much more higher and the behavior exhibited unusual strain hardening period starting at a strain of ~0.2. Note that similar tests have been carried out for composite pyramidal lattice structure in which the stacking sequence was $[0_2/90_2]$, and no trend of increasing strength was noted in the plateau region. Instead, the stress decreased as the strain increased, although failure also occurred by hollow trusses fracture [18]. Therefore, we

Table 1
Summary of the measured parameters for composite tubes in the improved design under compression.

d_o (mm)	d_i (mm)	Stacking sequence	Density of hollow truss ρ_s (g/mm^3)	Predicted relative density $\bar{\rho}_h$ (%)	Measured relative density $\bar{\rho}_h$ (%)	Modulus (GPa)	Strength (MPa)
6	5.4	$[(0, 90)]$	1.33	1.23	1.07	10.15	93.11
6	4.5	$[0_2/(0, 90)]$	1.4	2.82	2.21	11.66	121.32
6	3	$[0_4/(0, 90)_2]$	1.375	4.84	4.53	13.52	188.68

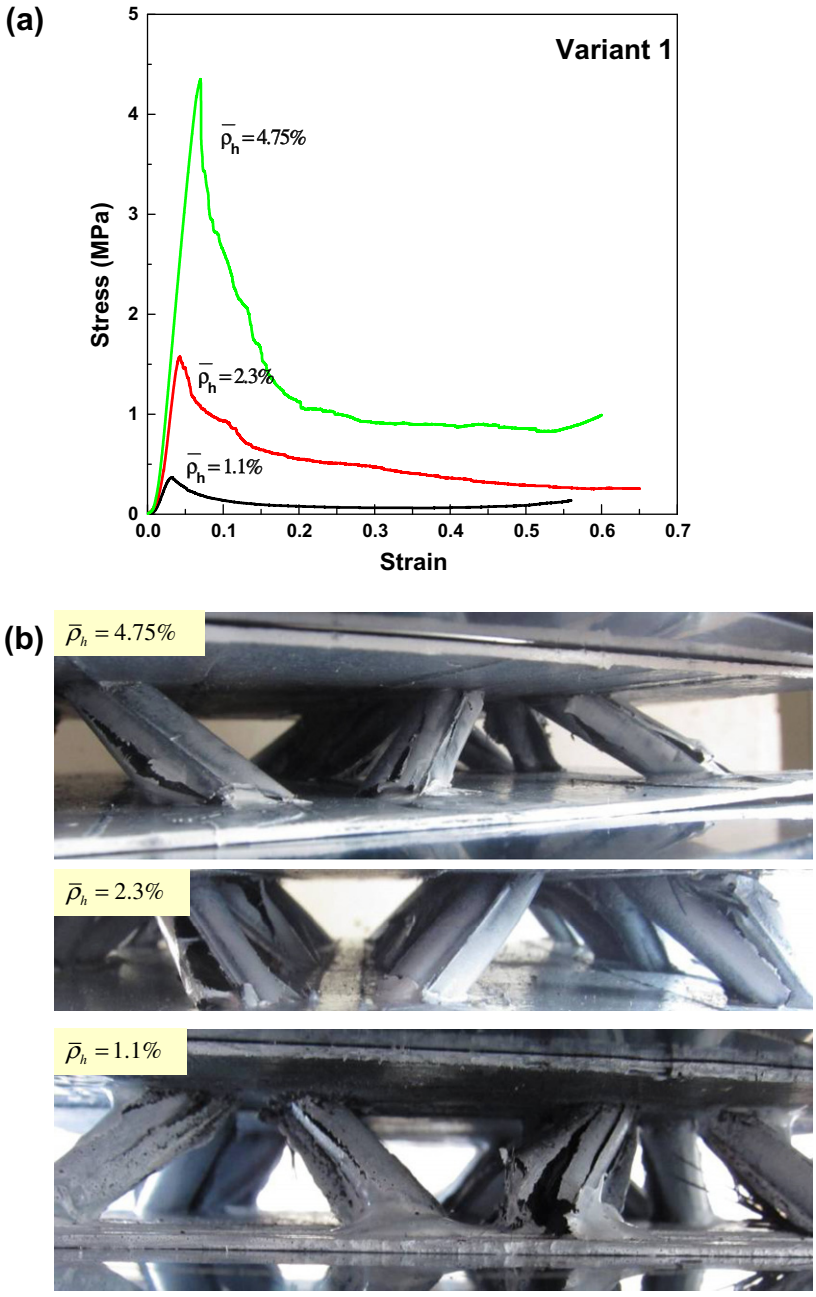

Fig. 4. Out-of-plane compressive responses and failure modes of hollow truss composite pyramidal lattice structures in Variant 1. (a) Compressive stress–strain curves. (b) Failure modes.

concluded that the incorporation of woven fabrics in the hollow truss lattice structures caused the observed increase in strength. Note that woven fabrics are also likely to enhance energy absorption [19].

The compressive modulus and peak strength of composite lattice structures are plotted against $\bar{\rho}_h$ in Fig. 6 and compared with the results from the initial approach. For purposes of analysis, we introduce a factor $\xi = n_a/n$, where n_a is the number of plies for axially aligned carbon fibers. Note that $\xi = 1$ in Variants 1a–c. In the [(0, 90)] case, the hollow trusses are comprised of plain weave fabric, and ξ for the pyramidal lattice core is 0.5. This value is half of the ξ value for the $[0]_2$ case, although the compressive modulus and strength are nearly identical. For the $[0_2/(0, 90)]$ and $[0_4/(0, 90)_2]$ cases, the average strength and modulus are slightly greater than the $[0]_5$ and $[0]_{10}$ structures. The above results show that pyramidal lattice structures with hollow composite trusses exhibit superior compressive modulus and strength when circumferentially oriented CF is incorporated to reinforce the truss members.

3.3. Column performance

The mechanical properties of composite tubes with different stacking sequences will vary according to the particular fiber architecture, and thus tube properties were measured separately. A similar steel mold was used to fabricate a single straight tube sandwich, and the tube ends were embedded into the facesheets in the same manner as their corresponding pyramidal lattice sandwich structures. Out-of-plane compression tests were carried out using the same displacement rate of 0.5 mm/min to determine

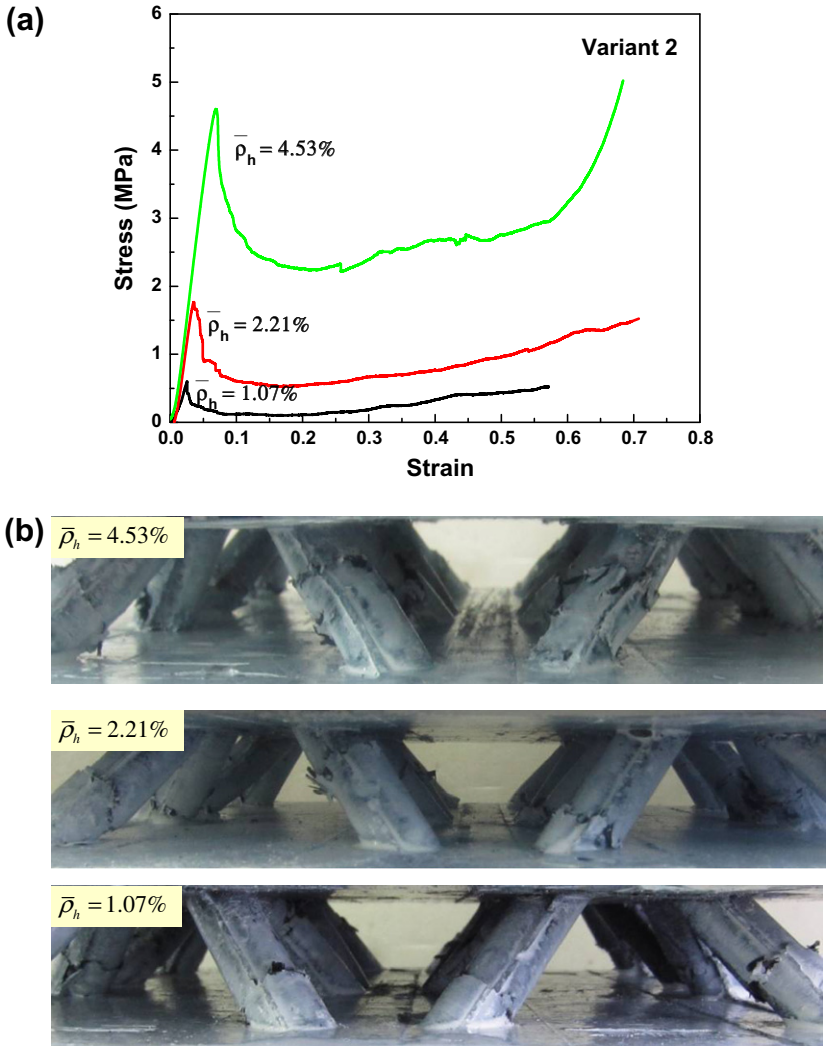

Fig. 5. Out-of-plane compressive responses and failure modes of hollow truss composite pyramidal lattice structures in Variant 2. (a) Compressive stress–strain curves. (b) Failure modes.

the compressive modulus and strength of these composite tubes for Variants 2a–c. The load–deformation curves are shown in Fig. 7b. In general, as the number of plies was increased, the modulus and the strength increased, as summarized in Table 1. Moreover, the peak strength of Variant 2a surpassed that of the solid truss composite lattice structures of comparable relative density [16], where Euler buckling controlled failure (Table 2).

4. Discussion

Hollow trusses are expected to enhance buckling resistance because of the larger radius of gyration $\sqrt{I/A}$ compared to solid counterparts [8]. Thus, the buckling strength of pyramidal lattice structures composed of hollow composite trusses will increase (relative to solid trusses of similar dimensions). Rules of strength will change from fracture to buckling when the density is sufficiently small [20–22]. The out-of-plane compressive properties of pyramidal lattice structures comprised of hollow composite trusses will be deduced in the following section. Euler buckling and fracture of composite tubes will be considered as two major competing failure modes. We will assume that each truss is rigidly attached to the face sheets so that the truss ends have clamped boundary conditions.

4.1. Compressive modulus

A theoretical analysis of the effective compressive modulus of hollow truss composite pyramidal lattice structure was undertaken by analyzing the deformation of a single tube, as sketched in Fig. 8. For an imposed displacement δ in the Z-direction, the axial and shear force, F_a and F_s, in the composite tube are given as

$$F_a = E_{cf}\frac{\pi\left(d_o^2 - d_i^2\right)}{4}\frac{\delta\sin\omega}{l_1} \tag{4}$$

$$F_s = \frac{12E_{cf}I\delta\cos\omega}{l_1^3} \tag{5}$$

where the second area moment $I = \pi\left(d_o^4 - d_i^4\right)/64$ and E_{cf} is the compressive modulus of composite tubes. The total force F in the Z-direction follows as

$$\begin{aligned} F &= F_a\sin\omega + F_s\cos\omega \\ &= \frac{E_{cf}\pi\left(d_o^2 - d_i^2\right)\delta}{4l_1}\left[\sin^2\omega + \frac{3}{4}\frac{d_o^2 + d_i^2}{l_1^2}\cos^2\omega\right] \end{aligned} \tag{6}$$

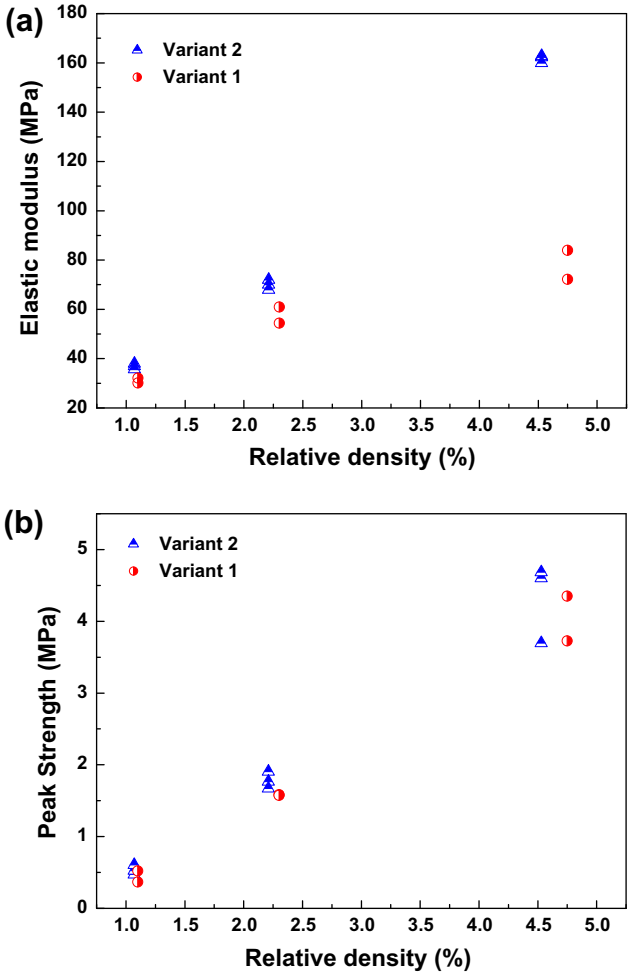

Fig. 6. Experimental measurements of (a) nominal compressive modulus and (b) peak compressive strength versus relative density of hollow truss composite lattice cores (Variants 1a–c and 2a–c).

Considering the unit cell of the hollow truss pyramidal core as sketched in Fig. 3, the nominal compressive modulus can be expressed as

$$E = E_{cf}\bar{\rho}_h \sin^4\omega + \frac{3}{4}E_{cf}\bar{\rho}_h \frac{d_o^2 + d_i^2}{l_1^2}\sin^2\omega\cos^2\omega \quad (7)$$

The first and second terms in Eq. (7) represent the stiffness of the pyramidal lattice core contributed by stretching and bending of the tubes, respectively. The aspect ratio is low, so the bending contribution could not be neglected.

4.2. Compressive strength

A force balance along the compression axis can be used to derive an equation relating the peak strength of the pyramidal unit cell to the failure stress of the individual truss [12]. The peak strength σ_p of a composite pyramidal lattice core with composite tubes is expressed as

$$\sigma_p = \sigma_c\bar{\rho}_h \sin^2\omega + \frac{3}{4}\sigma_c\bar{\rho}_h \frac{d_o^2 + d_i^2}{l_1^2}\cos^2\omega \quad (8)$$

where σ_c is the maximum compressive stress of hollow trusses.

For lattice structures composed of hollow trusses with medium-to-high slenderness ratios, the failure stress σ_c will be replaced by the critical buckling stress σ_{cb} as

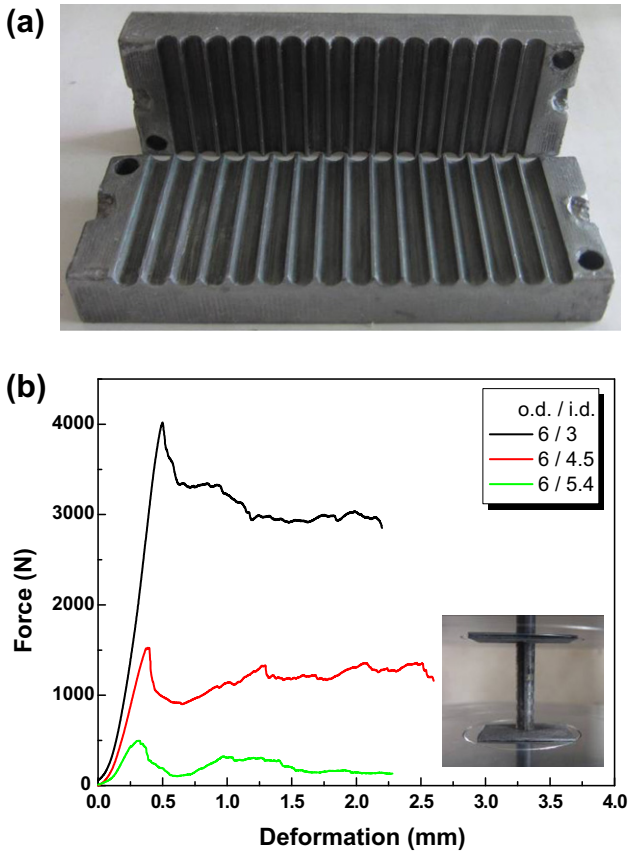

Fig. 7. (a) steel molds for fabricating single straight tube sandwich and (b) compressive load–deformation curves for three kinds of composite tube sandwiches in Variant 2.

$$\sigma_{cb} = \pi^2 E_{cf}\frac{d_o^2 + d_i^2}{4l_1^2} \quad (9)$$

Note that the stress for the onset of buckling in Eq. (9) is minimized when the trusses are solid ($d_i = 0$).

A truss that is relatively short and thick will fail by fracture of the composite tube, such that $\sigma_c = \sigma_{cf}$, where σ_{cf} is the fracture strength, often obtained by direct measurement rather than by the predictions of particular micromechanical models. Similarly, σ_{cf} is expected to vary for composite tubes with different numbers of plies and stacking sequences.

In the present study, lattice structures failed by fracture of composite tubes in all cases for Variants 2a–c. The comparison between theoretical predictions and experimental results are summarized in Table 2.

4.3. Impact energy absorption

The stress–strain curves for impact energy absorbing structures typically exhibit a long stress plateau with little or no work hardening [9]. The strain energy absorbed during compression up to the onset of densification can be used as a figure of merit to compare different cellular structures for impact energy absorption [23]. The energy absorption capacity per unit volume, W_v, is defined from the area under the nominal stress–strain curve as

$$W_v = \int_0^{\varepsilon_D} \sigma\, d\varepsilon \quad (10)$$

where the densification strain, ε_D, is taken to be the strain at which the stress re-attains its initial peak strength value (about 55–65% as

Table 2
Comparison between experimental data and theoretical prediction.

Samples	Relative density $\bar{\rho}_h$ (%)	Failure mode	Predicted modulus (GPa)	Measured modulus (GPa)	Predicted strength (MPa)	Measured strength (MPa)
Variant 2a	1.07	Fracture	30.47	35.72	0.56	0.60
Variant 2b	2.21	Fracture	71.21	72	1.48	1.91
Variant 2c	4.53	Fracture	166.03	160	4.63	4.68
Solid truss composite lattices [16]	1.25	Euler buckling	–	–	–	0.304

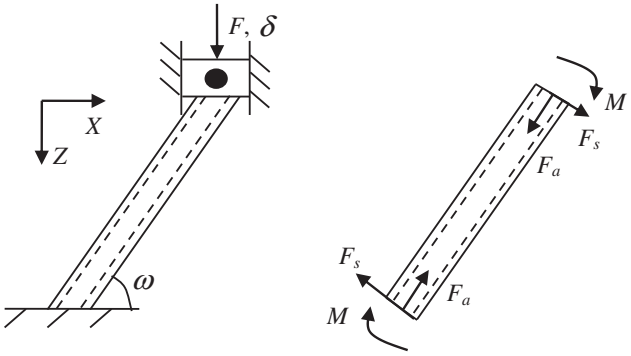

Fig. 8. The loading and boundary conditions of a single composite tube in *Z*-direction.

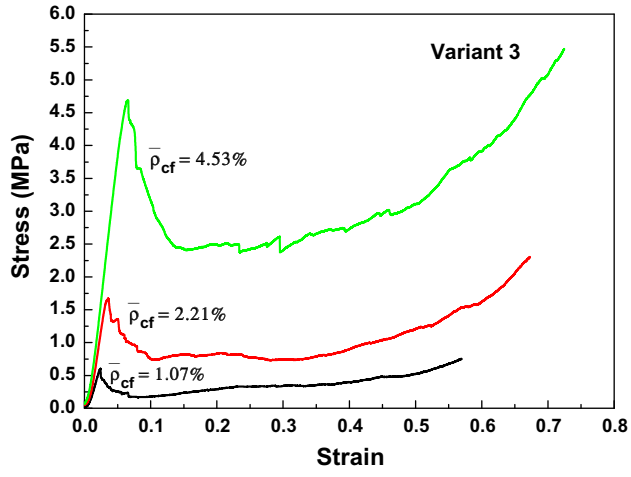

Fig. 9. Out-of-plane compressive responses of the corresponding rubber–core truss pyramidal lattice structures (Variants 3a–c).

shown in Figs. 5a and 9). The corresponding energy absorption per unit mass W_m is given by [9]

$$W_m = W_v/(\bar{\rho}\rho_{cf}) \quad (11)$$

Because of the addition of woven composites in Variants 2a–c and the resulting strain hardening period in the nominal stress–strain curves (Fig. 5a), the energy absorption capacity will also increase. The hybrid truss composite lattice structures (Variants 3) are similarly constructed and the silicone rubber in the truss is not removed. These rubber–core truss structures were reportedly potential candidates for impact protection and fabricated here using the same stacking sequences as those in Variants 2a–c.

The out-of-plane compressive stress–strain curves for Variants 3a–c are shown in Fig. 9. The curves exhibit characteristics similar to those of Variants 2a–c, including the strain hardening period in the plateau region. Here, $\bar{\rho}_{cf}$, representing the relative density fraction occupied by CF composites in the hybrid truss composite lattice structure, is equal to $\bar{\rho}_h$ for Variants 2a–c. As analyzed in [18], the compressive modulus and peak strength values for Variants 3a–c were similar to those of Variants 2a–c, primarily because of the much greater stiffness and strength of CF composites in the hybrid truss relative to those of the embedded rubber. The constrained silicone rubber inside the truss resisted the compressive deformation of the lattice structure and contributed to the observed strain hardening.

The energy absorption per unit volume and per unit mass for hollow truss and hybrid truss pyramidal lattice structures are shown in Fig. 10, and compared with hollow truss metallic lattice

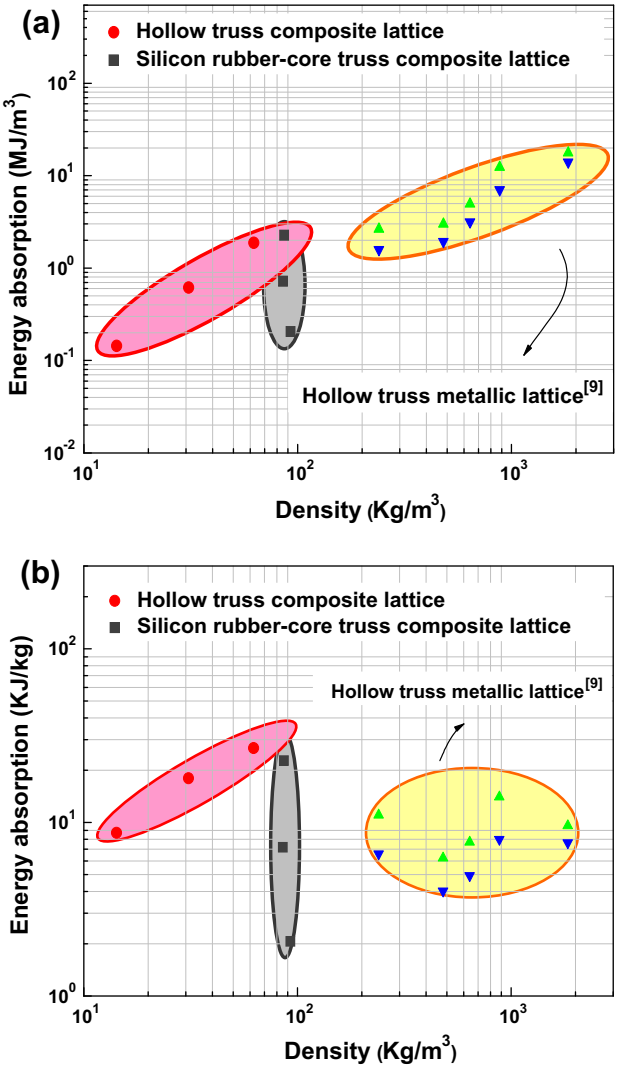

Fig. 10. Energy absorption (a) per unit volume and (b) per unit mass of selected hollow truss composite pyramidal lattice structures (Variant 2) comparing with those of the corresponding rubber–core truss composite pyramidal lattice structures (Variant 3) and hollow truss metallic lattice structures.

structures [9]. Fig. 10a shows that the energy absorption per unit volume of hollow truss composite lattice structures for Variant 2 were comparable to those of silicone rubber–core truss counterparts, but less than those of hollow truss metallic lattice structures. However, the corresponding energy absorption per unit mass of the hollow truss composite lattice structures was greater than those of hybrid truss composite lattice structures, and greater than hollow truss metallic lattice structures (Fig. 10b). Note that metallic lattice structures with hollow trusses are superior energy absorption candidates for cellular metal structures [9]. Nevertheless, the pyramidal lattice structures with hollow composite trusses reported here exhibit promising impact protection characteristics, particularly for weight-critical structures, and effectively expand the material property space for structural designers.

5. Conclusions

Pyramidal lattice core sandwich structures with hollow CF composite trusses were fabricated using a thermal expansion molding technique. The relative density of the composite lattice structure was controlled by the number of plies that comprised the composite tubes. One variant (Variant 1) for hollow truss lattice structures featured 100% uniaxial CF reinforcement axially aligned along the composite truss members, while a second variant (Variant 2) featured a fraction of CF oriented circumferentially. The elastic modulus and peak compressive strength of Variant 2 slightly exceeded those of Variant 1, because the failure mode changed from fiber splitting to tube fracture for Variant 2. The compressive strength tested here surpassed that of solid truss pyramidal lattice structure when Euler buckling used to control failure in [16]. Moreover, it might provide a possible route to improve the out-of-plane compressive properties of composite lattice structures in the present study by further optimization of stacking sequences of plies comprising the hollow trusses, since there still remains space comparing with the compressive modulus and strength of solid truss composite lattice structures [16].

Variant 2 exhibited more extensive strain hardening, which naturally led to increased energy absorption, both per unit volume and per unit mass. When compared with the energy absorption capacity of similarly constructed hybrid truss counterparts (Variant 3) and other competing lattice structures, the energy absorption per unit volume of composite lattice structures for Variants 2 and 3 were comparable, but slightly less than those of hollow truss metallic lattice structures. However, the energy absorption and compressive properties could be further increased by optimization mentioned above. The corresponding energy absorption per unit mass among the three kinds of structures considered is greatest for Variant 2. Because of this, the composite pyramidal lattice structures described here are promising candidates for impact protection, particularly in weight-sensitive structural applications.

Acknowledgments

The present work is supported by NSFC (90816024 and 10872059), 973 Program (No. 2011CB610303), Program for NCET (NCET-08-0152), Program of Excellent Team in HIT and the Fundamental Research Funds for the Central Universities (Grant No. HIT. KLOF2010029). S.N. gratefully acknowledges support from the M.C. Gill Composites Center. S.Y. also gratefully acknowledges the supports of Most Promising New Scholar Award (AUDQ1010000511).

References

[1] Evans AG, Hutchinson JW, Fleck NA, Ashby MF, Wadley HNG. The topological design of multifunctional cellular metals. Prog Mater Sci 2001;46(3–4):309–27.
[2] Kooistra GW, Deshpande VS, Wadley HNG. Compressive behavior of age hardenable tetrahedral lattice truss structures made from aluminium. Acta Mater 2004;52(14):4229–37.
[3] Deshpande VS, Fleck NA, Ashby MF. Effective properties of the octet-truss lattice material. J Mech Phys Solids 2001;49(8):1747–69.
[4] Zok FW, Waltner SA, Wei Z, Rathbun HJ, McMeeking RM, Evans AG. A protocol for characterizing the structural performance of metallic sandwich panels: application to pyramidal truss cores. Int J Solids Struct 2004;41(22–23):624971.
[5] Biagi R, Bart-Smith H. Imperfection sensitivity of pyramidal core sandwich structures. Int J Solids Struct 2007;44(14–15):4690–706.
[6] Wang J, Evans AG, Dharmasena K, Wadley HNG. On the performance of truss panels with Kagome cores. Int J Solids Struct 2003;40(25):6981–8.
[7] Rathbun HJ, Zok FW, Waltner SA, Mercer C, Evans AG, Queheillalt DT, et al. Structural performance of metallic sandwich beams with hollow truss cores. Acta Mater 2006;54(20):5509–18.
[8] Queheillalt DT, Wadley HNG. Pyramidal lattice truss structures with hollow trusses. Mater Sci Eng A 2005;397(1–2):132–7.
[9] Queheillalt DT, Wadley HNG. Cellular metal lattices with hollow trusses. Acta Mater 2005;53(2):303–13.
[10] Fan HL, Fang DN, Chen LM, Dai Z, Yang W. Manufacturing and testing of a CFRC sandwich cylinder with Kagome cores. Compos Sci Technol 2009;69(15–16):2695–700.
[11] Fan HL, Jin FN, Fang DN. Characterization of edge effects of composite lattice structures. Compos Sci Technol 2009;69(11–12):1896–903.
[12] Finnegan K, Kooistra G, Wadley HNG, Deshpande VS. The compressive response of carbon fiber composite pyramidal truss sandwich cores. Int J Mater Res 2007;98(12):1264–72.
[13] Russell BP, Deshpande VS, Wadley HNG. Quasistatic deformation and failure modes of composite square honeycombs. J Mech Mater Struct 2008;3(7):1315–40.
[14] Moongkhamklang P, Deshpande VS, Wadley HNG. The compressive and shear response of titanium matrix composite lattice structures. Acta Mater 2010;58(8):2822–35.
[15] Wang B, Wu LZ, Ma L, Sun YG, Du SY. Mechanical behavior of the sandwich structures with carbon fiber-reinforced pyramidal lattice truss core. Mater Des 2010;31(5):2659–63.
[16] Xiong J, Ma L, Wu L, Wang B, Vaziri A. Fabrication and crushing behavior of low density carbon fiber composite pyramidal truss structures. Compos Struct 2010;92(11):2695–702.
[17] ASTM: C365/C364M-05. Standard test method for flat wise compressive properties of sandwich cores. Weat Conshohocken (PA): ASTM Int.; 2006.
[18] Yin S, Wu LZ, Ma L. Hybrid truss concepts for carbon fiber composite lattice structure. Unpublished results.
[19] Harte AM, Fleck NA, Ashby MF. Energy absorption of foam-filled circular tubes with braided composite walls. Eur J Mech A-Solids 2000;19(1):31–50.
[20] Fan HL, Jin FN, Fang DN. Uniaxial local buckling strength of periodic lattice composites. Mater Des 2009;30(10):4136–45.
[21] Fan HL, Jin FN, Fang DN. Mechanical properties of hierarchical cellular materials. Part I: analysis. Compos Sci Tech 2008;68(15–16):3380–7.
[22] Fan HL, Fang DN. Enhancement of mechanical properties of hollow-strut foams: analysis. Mater Des 2009;30(5):1659–66.
[23] Ashby MF et al. Metal foams: a design guide. Woburn (MA): Butterworth–Heinemann; 2000.